Since January 2020 Elsevier has created a COVID-19 resource centre with free information in English and Mandarin on the novel coronavirus COVID-19. The COVID-19 resource centre is hosted on Elsevier Connect, the company's public news and information website.

Journal of Hazardous Materials 167 (2009) 736–744

Contents lists available at ScienceDirect

Journal of Hazardous Materials

journal homepage: www.elsevier.com/locate/jhazmat

Numerical modeling of exhaled droplet nuclei dispersion and mixing in indoor environments

K.W. Mui [a], L.T. Wong [a], C.L. Wu [b], Alvin C.K. Lai [b,*]

[a] Department of Building Services Engineering, The Hong Kong Polytechnic University, Hung Hom, Kowloon, Hong Kong
[b] Department of Building and Construction, City University of Hong Kong, Tat Chee Avenue, Kowloon, Hong Kong

ARTICLE INFO

Article history:
Received 15 October 2008
Received in revised form 11 January 2009
Accepted 12 January 2009
Available online 20 January 2009

Keywords:
Particle dispersion
Drift-flux model
Mixing
Ventilation

ABSTRACT

The increasing incidence of indoor airborne infections has prompted attention upon the investigation of expiratory droplet dispersion and transport in built environments. In this study, a source (i.e. a patient who generates droplets) and a receiver (i.e. a susceptible object other than the source) are modeled in a mechanically ventilated room. The receiver's exposure to the droplet nuclei is analyzed under two orientations relative to the source. Two droplet nuclei, 0.1 and 10 μm, with different emission velocities, are selected to represent large expiratory droplets which can still be inhaled into the human respiratory tracts. The droplet dispersion and mixing characteristics under well-mixed and displacement ventilation schemes are evaluated and compared numerically. Results show that the droplet dispersion and mixing under displacement ventilation is consistently poorer. Very low concentration regions are also observed in the displacement scheme. For both ventilation schemes, the intake dose will be reduced substantially if the droplets are emitted under the face-to-wall orientation rather than the face-to-face orientation. Implications of using engineering strategies for reducing exposure are briefly discussed.

1. Introduction

Humans spend over 85% of their time in confined microenvironments, i.e. transport, workplace, and residence [1]. The apparent importance of controlling airborne transmission of infectious agents in indoor environments is well recognized. However, detailed understanding of the airborne behavior of infectious agents in these environments is still far from complete.

Today, controlling and reducing human-to-human airborne transmission of highly contagious pathogens including Severe Acute Respiratory Syndrome (SARS), tuberculosis, and other multidrug resistant strains is a growing concern. Significant efforts, in addition to those spent in extensive life science researches, have been devoted to propose engineering control strategies that reduce airborne infection risks [2]. To develop any successful and practical strategies or policies, it is imperative to gain more knowledge about the physical behaviors of airborne droplets in indoor environments [3–9] and the roles of ventilation schemes in airborne transmissions [10,11].

When a contagious individual (the source) coughs or sneezes, droplets containing infectious microorganisms (bacteria, viruses) are released. The moist coating of saliva and mucus will evaporate, leaving a residual dry nucleus of the droplet that may include one or more bacteria or viruses. The dried droplets are called droplet nuclei and are responsible for human-to-human transmission of the airborne infectious pathogens. Although the exact mechanism underlying droplet nuclei infection is not fully understood, it is known that the first step in a series of dose–response relations leading to the infection is the regional deposition of inhaled particles in the lung. Generally speaking, the intake dose (or called the exposure dose) is a function of both temporal and spatial droplet nuclei concentration which depends on the physical characteristics of the nuclei such as droplet sizes and airflow patterns, as well as many environmental factors including relative source-to-receiver locations.

Airflow pattern is the most significant parameter influencing the droplet transport in indoor environments [4,10–13]. The choice of ventilation scheme controls the global airflow pattern and thus the ultimate distribution of pollutants. There are two ventilation schemes being widely used in commercial offices, viz. the conventional well-mixed (or ceiling supply and return) ventilation–high velocity cooled air is delivered through high ceiling/side wall supply diffusers, and the displacement ventilation–low momentum cooled air is supplied to the lower part of the space [14–15]. For both of these schemes, the exhausts are normally located on the high ceilings. A recent study has shown that the uni-directional upward ventilation system is more efficient in removing small droplets while the single floor system is more efficient in removing large droplets [16].

* Corresponding author. Tel.: +852 3442 6299; fax: +852 2788 7612.
E-mail address: alvinlai@cityu.edu.hk (A.C.K. Lai).

0304-3894/$ – see front matter © 2009 Elsevier B.V. All rights reserved.
doi:10.1016/j.jhazmat.2009.01.041

Expiratory droplets can be classified as coarse and fine aerosols. Coarse aerosols do not become truly airborne as they settle onto the floor rapidly after emission, whereas fine aerosols remain airborne for a prolonged period because of their low settling velocity and lead to a high potential for long-range infections [17]. Preliminary studies show that droplet size is one key factor affecting the spread of droplet nuclei. An updated review has summarized three past studies (spanned over the last five decades) on the sizes of particles emitted during coughing or sneezing [6]. It has been reported that for droplets less than 50 μm, the dispersion feature is dominant due to the very short evaporation time [18,19]. Hence, in this work, evaporating was not considered and two droplet nuclei sizes, 0.01 and 10 μm, corresponding to fine and coarse nuclei for viral and bacteria infections, respectively, were chosen. Another key factor is the droplet emission velocity. Reportedly, the initial emission velocity can be up to 100 m/s [20]. A recent study on coughed airflows of healthy males showed that the emission velocity was in the range of 6–22 m/s [21]. Based on these results, three velocities namely 20, 50 and 100 m/s were selected for this work. Breathing will also disturb the airflow pattern. However, due to the relatively small airflow volume when breathing, the exhaling process is believed to have little influence on the room airflow pattern [22]. Thus it was not considered in the present work.

When coughing or sneezing, the source is very often not facing other persons directly. The relative orientation and distance between the source and the (susceptible) receiver plays an ultimate role in exposure levels [6]. Based on daily observation and engineering judgment, two source-to-receiver orientations were considered in this work: (1) the source facing the receiver directly (i.e. a face-to-face orientation); (2) the source facing a wall directly (i.e. a face-to-wall orientation). In reality, it is very unlikely that the source can turn more than 90° before an expiratory process commences. Therefore, it is anticipated that results from the face-to-face orientation represent maximal exposure level while those from the face-to-wall orientation give a (practical) minimal exposure.

The objectives of the present work are to study the dispersion characteristics of exhaled droplet nuclei and to quantify the degree of mixing for various emission/orientation scenarios.

2. Methods

2.1. Description of the geometry

An enclosure with two identical standing model occupants with heat dissipated was modeled. There is one source occupant emitting droplets and the other occupant is the receiver. The geometry of the human occupant used in this work was originally suggested by Brohus and Nielson [23]. To simulate the occupant's mouth, an opening at a height of 1.54 m was added to the centerline of the head. Two ventilation schemes were investigated. The only differences between the well-mixed and displacement ventilation configurations are the inlet boundary conditions, location and geometry. The outline of the face-to-wall orientation under well-mixed ventilation is shown in Fig. 1.

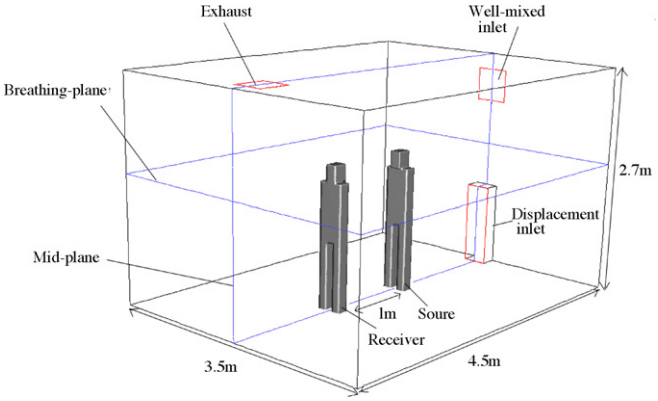

Fig. 1. Geometry of the test room for face-to-wall orientation.

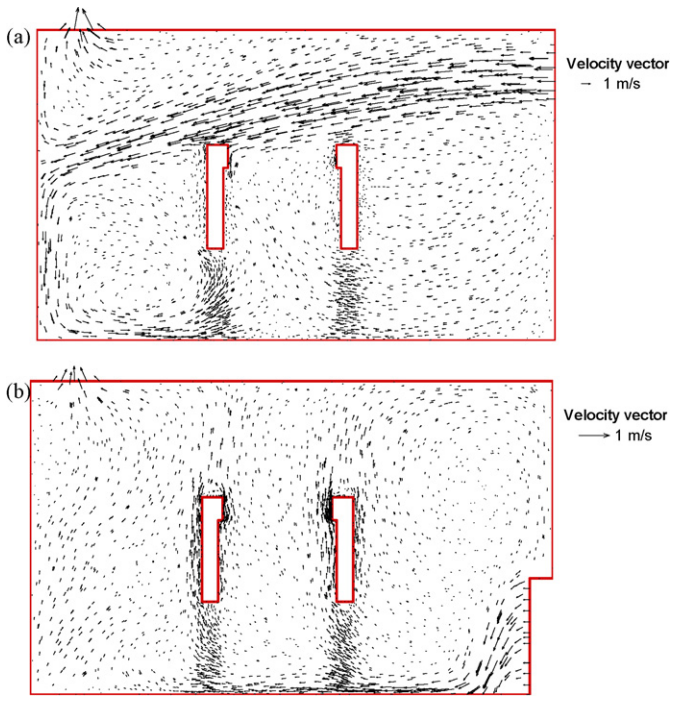

Fig. 2. Velocity magnitude at the mid-plane (a) well-mixed ventilation; (b) displacement ventilation.

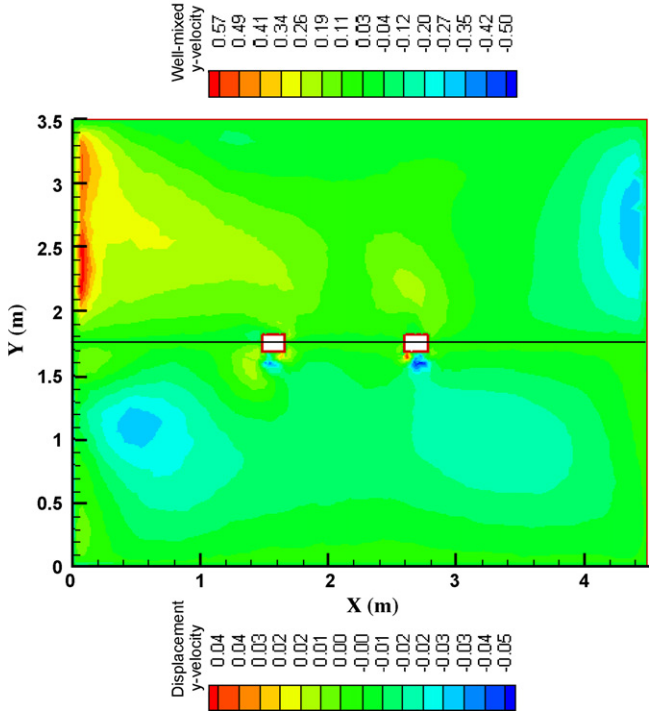

Fig. 3. *y*-Component velocity contour plots. The upper half shows the well-mixed ventilation and the bottom half shows the displacement ventilation.

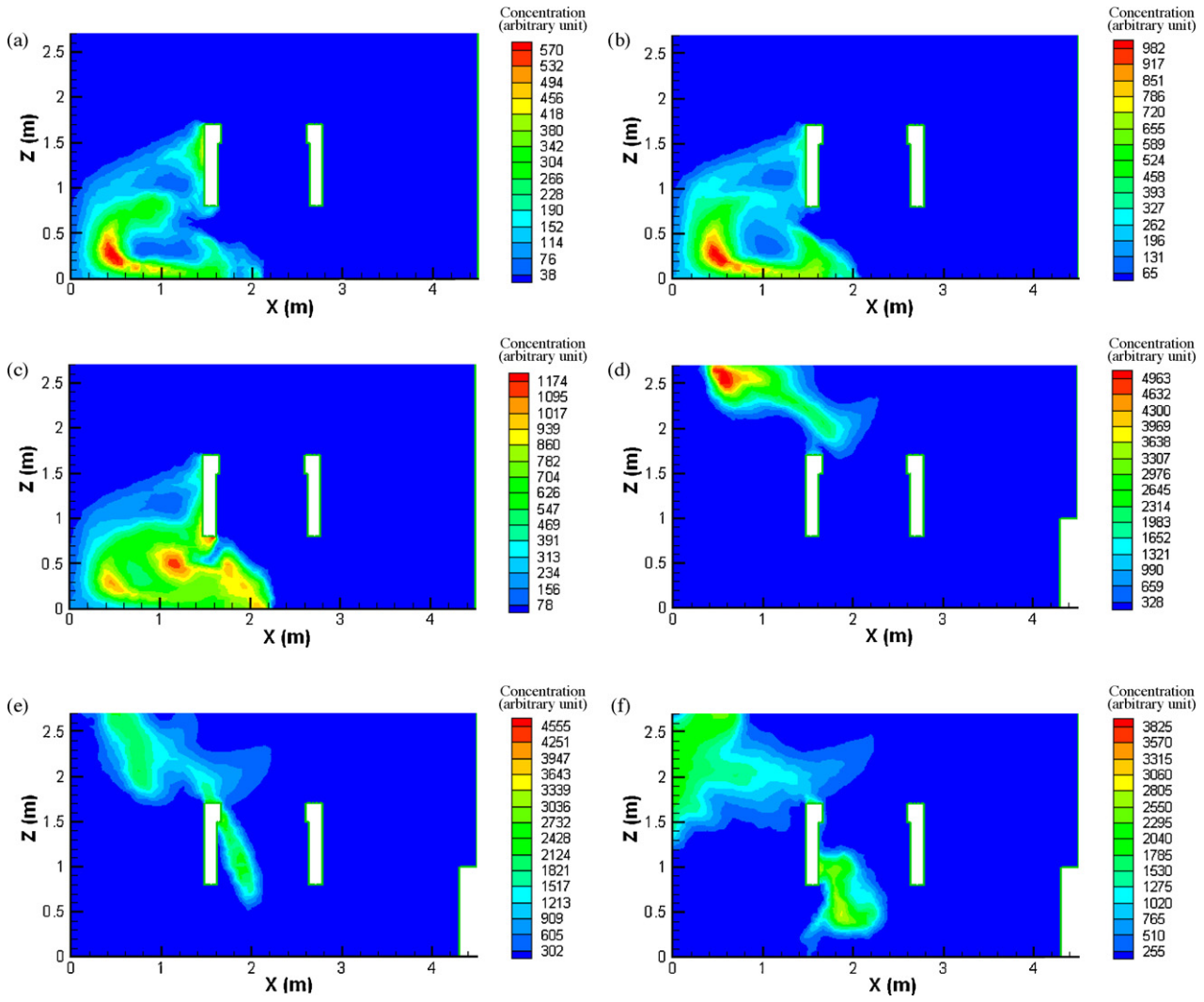

Fig. 4. Eulerian plots of 10 μm droplets at 10 s after emission for face-to-face orientation at mid-plane (a) well-mixed, 20 m/s; (b) well-mixed, 50 m/s; (c) well-mixed, 100 m/s; (d) displacement, 20 m/s; (e) displacement, 50 m/s; (f) displacement, 100 m/s.

2.2. Numerical modeling of airflow

One common methodology to resolve indoor two-phase problems is the Eulerain–Lagrangian approach, by which the airflow is modeled in a Eulerian framework while the droplet trajectories are traced individually. Recently, a drift-flux model developed by Chen et al. based on an Eulerian–Eulerian approach has been validated with a scaled experimental chamber [24,25]. The model incorporates a set of semi-empirical expressions to model aerosol deposition mechanism [26]. The deposition modeling takes Brownian diffusion, turbulent diffusion and gravitational settling into account, and has been widely applied to predict deposition for indoor environments [27,28], ventilation ducts [29,30] and lung bifurcations [31] since its first publication. The drift-flux model is descried briefly as follows.

Renormalization group (RNG) k-ε turbulent model was adopted to simulate the airflow. A generic commercial CFD code FLUENT was used in the simulation. The PISO algorithm was employed to couple the pressure and velocity fields. Grid independent tests were performed and for the face-to-face orientation, the optimal grid densities found for the well-mixed and displacement ventilation geometries were 404,000 and 375,000 cells, respectively. Similar cell numbers were used for the face-to-wall orientation. Details of the occupant and the inlet–outlet configurations can be found in an earlier study [10]. In brief, air inlet velocity was set to 2 m/s with a temperature of 14 °C, wall temperature was set to 25 °C and body temperature 36 °C was chosen for the well-mixed scheme while air inlet velocity and temperature were modified to 0.2 m/s and 19 °C, respectively. Higher than normal body temperature was selected as patient with fever was modeled. Since buoyancy flow was involved, air density was defined as a function of temperature by a piecewise-linear function. The simulation was performed on an SGI Onyx 3800 shared server.

2.3. Modeling of droplet nuclei transport

The drift-flux model, encoded into FLUENT through user-defined subroutines, was used to model transient droplet concentration distribution [24,25]. Due to the low volume fraction of indoor particles, one-way coupling was assumed. The governing equation for the droplet concentration can be written as:

$$\frac{\partial C_i}{\partial t} + \nabla \cdot \left[\left(\boldsymbol{u} + \mathbf{v}_{s,i}\right)\right] = \nabla \cdot \left[(D_i + \varepsilon_p)\nabla C_i\right] + S_{C_i} \quad (1)$$

where C_i is the particle concentration of a particle size group i (hereafter denoted via the subscription i), $\mathbf{v}_{s,i}$ is the particle settling velocity, $\varepsilon_{p,i}$ is the particle eddy diffusivity and D_i is the Brownian diffusion coefficient. For small particles it is assumed that $\varepsilon_p/\nu_t \approx 1$,

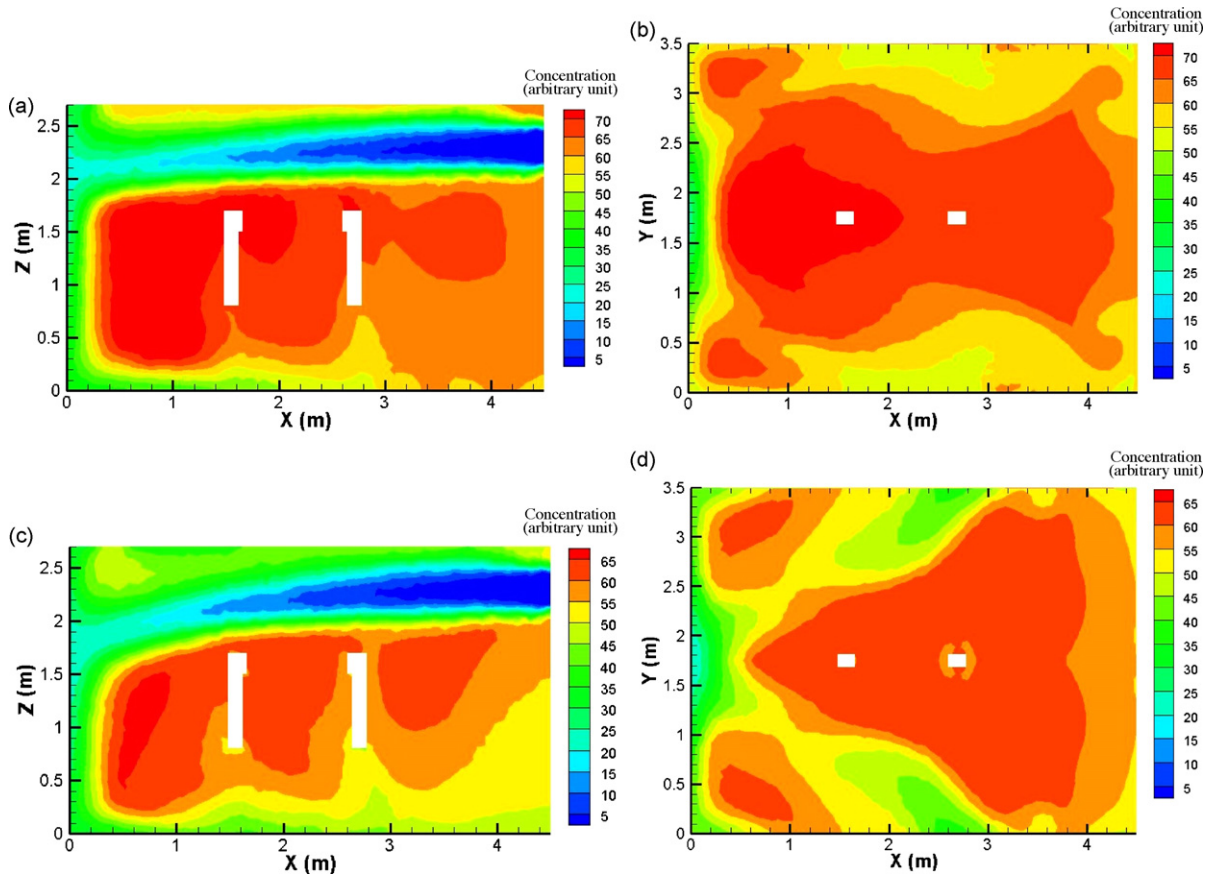

Fig. 5. Eulerian plots at 90 s after emission for face-to-face orientation under well-mixed ventilation with an emission velocity of 50 m/s (a) mid-plane, 0.01 μm; (b) breathing plane 0.01 μm; (c) mid-plane, 10 μm; (d) breathing plane, 10 μm.

where ν_t is the carrier fluid turbulent viscosity. Deposition of particles was modeled as a flux towards the wall. Through the semi-empirical expressions, the local deposition rate was evaluated [26].

For all the cases studied, a single episodic emission event which lasted for 0.5 s was selected and modeled. The droplet shape was assumed to be spherical with a density of 1000 kg/m^3. Simulation times specified for the well-mixed and displacement ventilation schemes were 90 and 240 s, respectively. The displacement scheme required a longer simulation time due to its lower air exchange rate. In either scheme, the droplet concentration decayed to a significantly low level when the specified time was reached and no significant reduction in concentration was found by further increasing the simulation time. A trapped boundary condition was applied for the droplets; once the particle touches any surfaces, it will not resuspend. For the present work, coagulation effect was not taken into account.

3. Results and discussion

3.1. Airflow pattern

Fig. 2 shows the steady state velocity plot of both ventilation schemes prior to the droplet emission at the mid-plane while the *y*-component velocity is shown in Fig. 3. According to these figures it is observed that under the well-mixed scheme a high velocity air jet, approximately equals the supply air whose velocity is 2 m/s, flows above both occupant models and causes a large eddy recirculation in the room. For the displacement scheme, it is noticed that the low velocity cooled air (0.2 m/s) near floor level absorbs heat from the two occupants and creates a dominant vertical thermal plume in the boundary layer around each occupant. The airflow velocity is fairly weak in all regions except at the mid-plane (Fig. 3). As will be discussed, this low velocity feature affects the overall droplet dispersion patterns.

3.2. Effects of ventilation on droplet dispersion and exposure level

Fig. 4 shows the concentration profiles at the mid-plane for various emission velocities under the face-to-face orientation. The plots are snapshots at 10 s after emission. Results reveal that there is no significant concentration difference among the three emission velocities in the well-mixed space (*c.f.* Fig. 4(a)–(c)). The particle relaxation time (τ) can be used to explain this observation. It is the time required for a particle to "relax" or to reach its terminal

Table 1
Surface and volume integrals of concentration of droplet nuclei for the two orientations.

	Breathing plane surface integral under well-mixed, in arbitrary unit		Breathing plane surface integral under displacement, in arbitrary unit		Volume integral under well-mixed, in arbitrary unit	Volume integral under displacement, in arbitrary unit
	0.01 μm	10 μm	0.01 μm	10 μm	0.01 μm	0.01 μm
Face-to-face	64.78	56.85	29.66	24.34	45445	114796
Face-to-wall	42.06	48.88	99.21	60.57	6059	15970

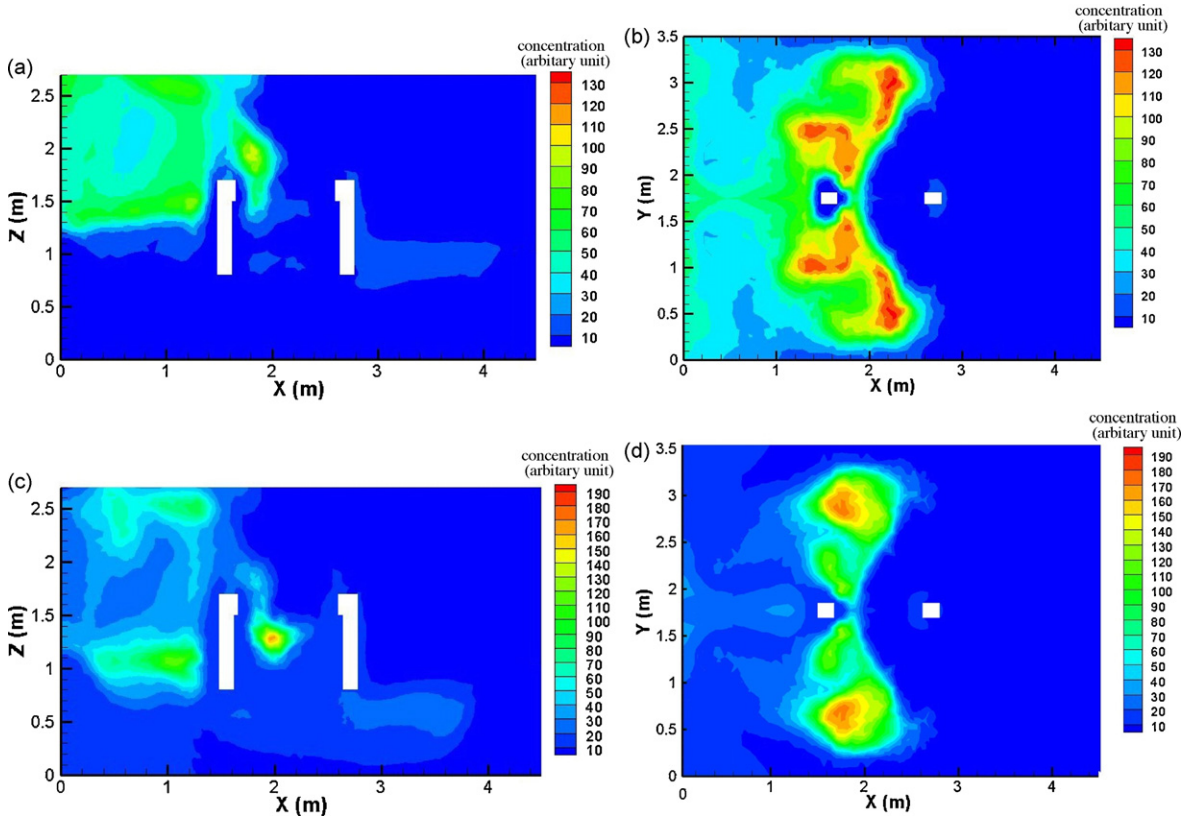

Fig. 6. Eulerian plots at 240 s after emission for face-to-face orientation under displacement ventilation with an emission velocity of 50 m/s (a) mid-plane, 0.01 μm; (b) breathing plane 0.01 μm; (c) mid-plane, 10 μm; (d) breathing plane, 10 μm.

velocity due to a sudden acceleration, and is defined as:

$$\tau = \frac{C_c d_p^2 \rho_p}{18\mu} \tag{2}$$

where C_c is the Cunningham slip correction factor and d_p is the droplet diameter. For the present scenarios, the droplet relaxation time is in the order of 10^{-4} s which can be neglected. In other words, the droplets decelerate almost instantaneously and that elucidates why the droplets follow the airflow closely–hence the similarity between the airflow and concentration profiles.

However, apparent concentration differences can be seen in the displacement ventilated space for various emission velocities. The higher the emission velocity from the source, the greater is the degree of particle impaction around the receiver (*c.f.* Fig. 4(d)–(f)). Intuitively, it contradicts with the previous discussion that particles with such a small relaxation time should follow the global airflow pattern closely regardless of the emission velocity. The difference is attributed to the finite emission duration together with low velocity background airflow. For the displacement case, the emission velocity is "significantly" higher comparing to the global airflow. This finite and high velocity droplet cloud leads to various impaction patterns around the receiver. If the particles were released instantly, the profiles should not be affected by the emission velocity.

The cases for a longer elapsed time under the emission velocity of 50 m/s were further explored. Figs. 5 and 6 depict the concentration profiles for the two chosen droplet nuclei sizes in the breathing plan as well as at mid-plane. Under the well-mixed scheme, well-mixed conditions can be achieved within 90 s after droplet emission as the airflow and the droplet cloud travel in the same direction (more quantitative analysis below). Under the displacement scheme, due to the lower global velocity, only moderate inhomogeneous concentration can be noticed even at 240 s after the emission. Low concentration regions (hereafter referred to droplet-free can be observed under the displacement scheme. One is identified at the air supply area (bottom right of Fig. 6(a)). Formed as a consequence of the removal characteristics of displacement ventilation, i.e. the warm, stale air ascends to the ceiling where it is exhausted through the outlet, the droplet-free area is observed. The (contaminated) vertical thermal plume makes the droplets less likely to disperse within the room. Compared with well-mixed ventilation, displacement ventilation has a much lower average eddy diffusivity (about 1/20 of the well-mixed's). The droplets, largely influenced by buoyant airflow, are less dispersed by the turbulence. Another droplet-free region exists on the rear side of the source and occupies almost half of the breathing plane (Fig. 6(b)). This can be attributed to the prevailing flow direction and very low transport velocity in that region (Fig. 2(b)).

Based on these findings, it can be concluded that the ultimate concentration profile is dependent on the ventilation scheme, global air velocity, relaxation time, as well as emission duration and velocity. Moreover, the results imply that in a displacement ventilated space, occupants behind the droplet source will be less likely infected. On the other hand, because of the large recirculation eddy, the probability of being infected is almost the same everywhere in the well-mixed flow environment (Fig. 5). Table 1 shows the averaged concentration (in arbitrary unit) for each breathing plane. Except for the face-to-wall orientation under the displacement ventilation scheme, droplet size differences are not significant. Hence, only results of the 0.01 μm particles were chosen for the homogeneity calculation below (Figs. 9–11).

Figs. 7 and 8 show the concentration profiles for the face-to-wall orientation. Under the displacement scheme, a large droplet-free zone in the upper region and fairly well-mixed concentration in the lower region can be observed. Comparing Figs. 5 and 7, it is also observed that under the well-mixed scheme, the contours for face-

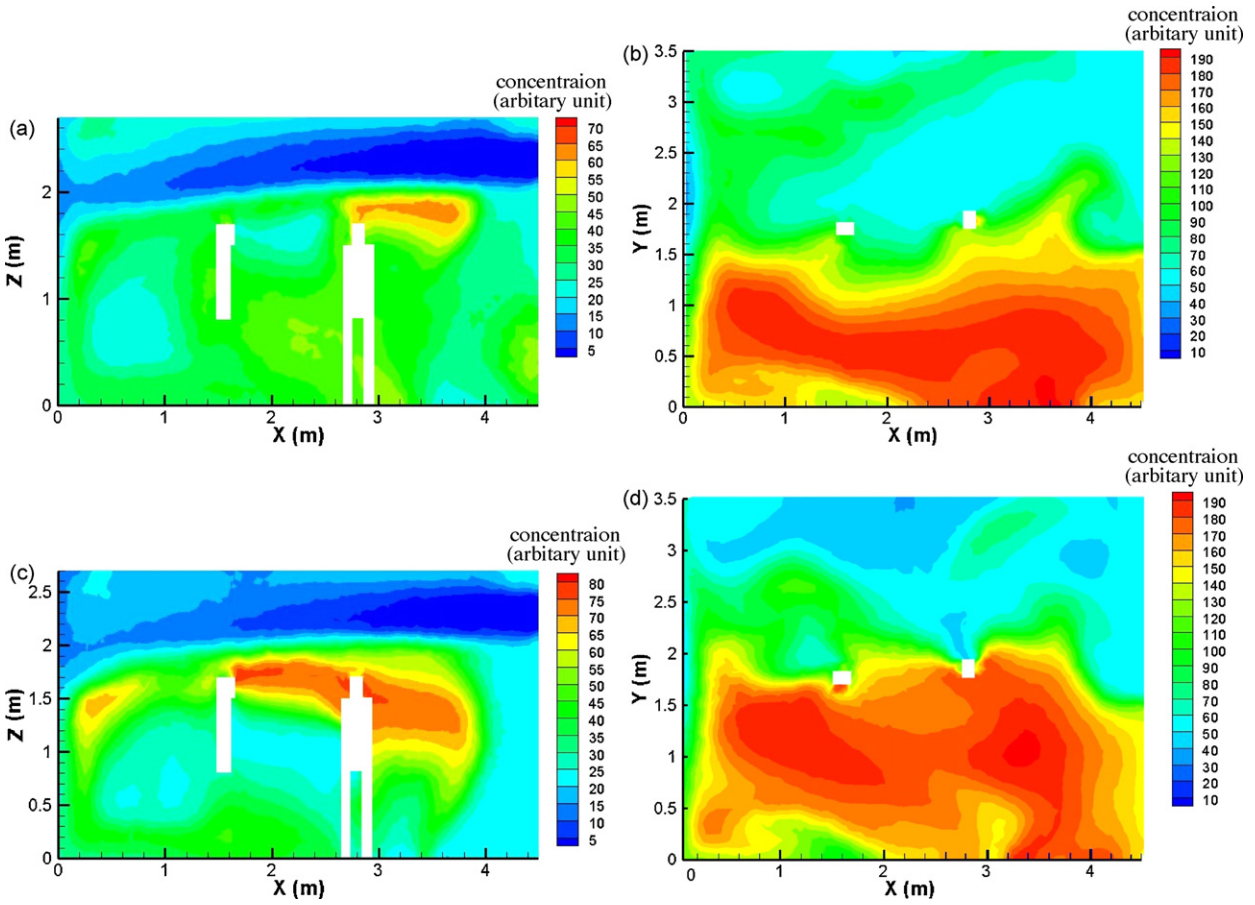

Fig. 7. Eulerian plots at 90 s after emission for face-to-wall orientation under well-mixed ventilation with an emission velocity of 50 m/s (a) mid-plane, 0.01 μm; (b) breathing plane 0.01 μm; (c) mid-plane, 10 μm; (d) breathing plane, 10 μm.

to-wall orientation exhibit inhomogeneity in the low concentration area (top of Fig. 7). The poor mixing between the upper and lower regions in both of the ventilation schemes can be attributed to the low convective transport in the *y*-direction (Fig. 3). This outcome reveals that in low airflow environments, the droplet emission direction can significantly influence the location of a droplet-free region and thus the degree of exposure level.

The infection risk depends strongly on the exposure which can be evaluated by $\int_0^T C(t)\mathrm{d}t$ – the total exposure from time 0 to the specified ending time T. Via this time integration, exposure levels were quantified for the 0.01 μm droplet nuclei. The values are tabulated in Table 1. These results show exposure can be reduced by more than 86% if it is a face-to-wall scenario.

3.3. Quantitative estimation of mixing

In the literature, there are some multi-zone indoor air quality computer programs developed to simulate contaminant transport in indoor environments, i.e. CONTAMW [32] and COMIS [33], apart from the research-orientated program developed to model multi-zone aerosol transport [34]. All of these programs assume uniform distribution of particles within each microenvironment and particles are transported by convective airflow only. All but one program ignore Brownian and turbulent diffusion for the transport mechanisms [34]. Figs. 5–8 clearly illustrate that the well-mixed assumption is over-simplified, particularly for the face-to-wall orientation. For certain airborne transmitted diseases, even inhalation of a small dose can cause infection [20,35]. To improve exposure assessment, more accurate predictions on the spatial concentration distribution (or exposure) and the mixing degree are highly desirable. More importantly, engineers can thereby design and implement better control strategies for reducing airborne pollutant concentration.

To represent the non-uniformity of a concentration field, the coefficient of variation $CV_i(t)$ defined as follows is adopted [36]:

$$CV_i(t) = \frac{1}{\overline{C_i}(t)}\sqrt{\frac{\sum_{i=1}^{N}\left(C_i(t)-\overline{C_i}(t)\right)^2}{N}} \quad (3)$$

where $\overline{C_i}(t)$ is the volume averaged concentration, $C_i(t)$ is the sampling point concentration at elapsed time t and N is the number of sample points. In the present work, the sampling points were taken at all of the computational cells; therefore, N is the number of cells.

Fig. 9 shows the CVs for both well-mixed and displacement schemes under the face-to-face orientation. In the former scheme, the three emission velocities collapse into a single line and that is consistent with the previous discussion on relaxation time. In the latter scheme, the CV depends on the emission velocity: the higher the emission velocity, the lower the CV (i.e. better mixing). Due to its higher global airflow velocity, as expected, well-mixed ventilation always has a lower (resulting) CV than displacement ventilation. Recent study has also shown that the higher velocity of well-mixed ventilation scheme resulted in faster mixing rate than with the displacement ventilation [37]. Another factor affecting the concentration is droplet deposition. The high airflow rate might also increase the particle deposition onto indoor surfaces [38,39] but for the particle sizes concerned in the present work, ventilation is still the dominant particle removal mechanisms.

Fig. 10 presents the CVs for both face-to-face and face-to-wall orientations under the well-mixed ventilation with an emission

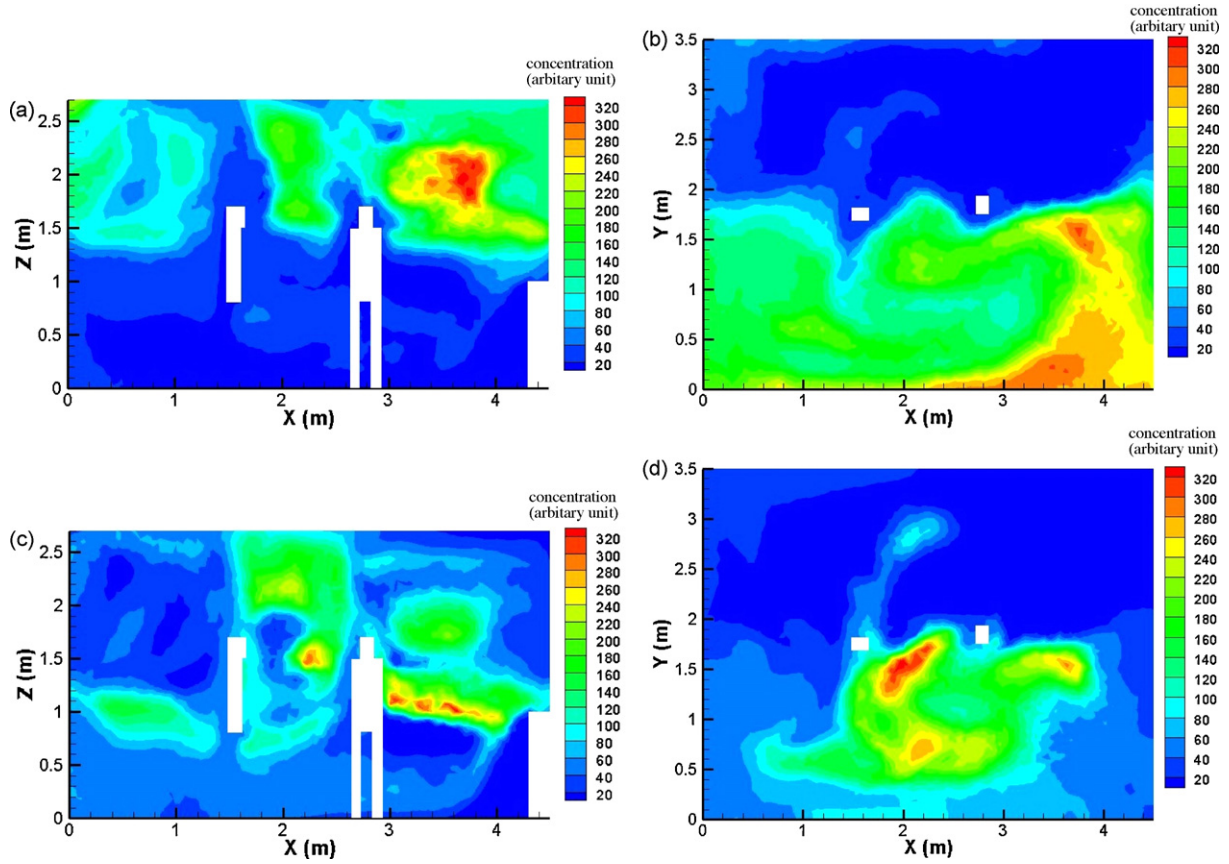

Fig. 8. Eulerian plots at 240 s after emission for face-to-wall orientation under displacement ventilation with an emission velocity of 50 m/s (a) mid-plane, 0.01 μm; (b) breathing plane 0.01 μm; (c) mid-plane, 10 μm; (d) breathing plane, 10 μm.

velocity of 50 m/s. Once again, the poor mixing characteristics of the face-to-wall orientation resulted in a higher CV by comparison with the face-to-face orientation (*c.f.* Figs. 5(b) and (d) and 7(b) and (d)). The CVs for the two orientations under the displacement ventilation with the same velocity are shown in Fig. 11. Comparing Figs. 10 and 11, it can be seen that the CV for the displacement ventilation is almost one order of higher than that for the well-mixed scheme.

It should be noted that all the CVs presented in this work are quite low on account of the nature of the emission. If the same well-mixed criterion by Mage and Ott [36] was applied, all the projected scenarios would be classified as "well-mixed" within seconds after the emission. However, this work simulates only a single coughing/sneezing event in a ventilated room. All the droplets in the simulated episodic events, unlike those in continuous injection, will eventually "disappear" inside the computational domain either by exiting through the exhaust system or depositing onto the indoor surfaces.

Generally speaking, droplets will be homogeneously mixed within a few minutes after emission under conventional well-mixed ventilation. On the contrary, very high concentration gradients will be observed under displacement ventilation. This essential difference between the concentration profiles forms the basis for

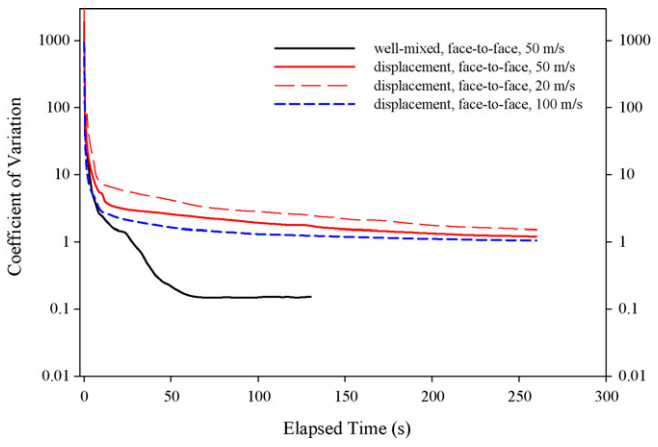

Fig. 9. Coefficient of variation of concentration field for face-to-face orientation under well-mixed and displacement ventilations.

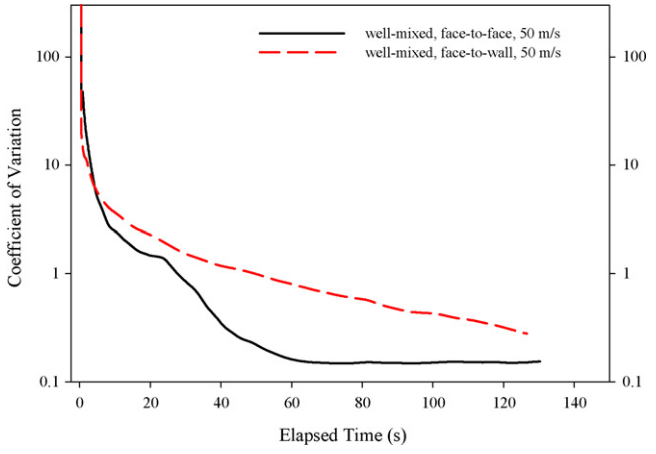

Fig. 10. Coefficient of variation of concentration field for face-to-face and face-to-wall orientations under well-mixed ventilation with an emission velocity of 50 m/s.

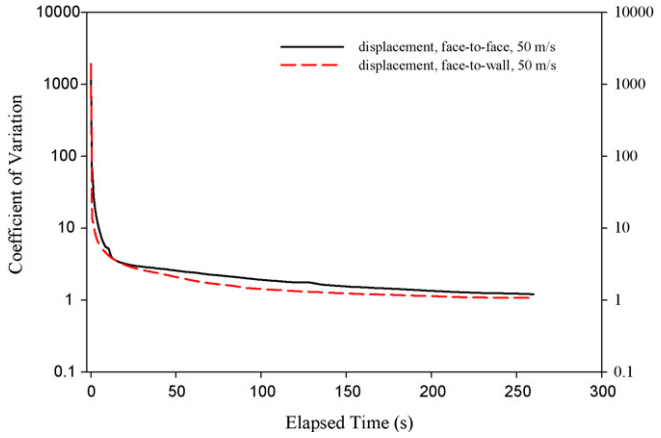

Fig. 11. Coefficient of variation of concentration field for face-to-face and face-to-wall orientations under displacement ventilation with an emission velocity of 50 m/s.

the implementation of engineering strategies for reducing exposure to airborne particles. Recently, many active devices for the removal of indoor pollutants have been designed and made available commercially. Technologies applied include high efficiency filtration, adsorption onto surfaces, inactivation by UV, and photocatalytic oxidation by titanium oxide. To effectively reduce the pollutants, the device should be installed at the location where high concentration exists. From the present findings, two major inferences can be drawn. First, the location of the active device is not a concern under any well-mixed ventilation schemes. Second, in order to achieve maximum pollutant removal efficacy under any displacement ventilation schemes, the active device should be installed near the exhaust outlet or high ceiling (*c.f.* Figs.6(a) and (c) and 8(a) and (c)). This can prevent further airborne infection by inactivating the droplets before they (if any) disperse back into the environment.

3.4. Constraints of the model

In this work, we modeled the occupants standing still. It is understood that in reality the occupants will move continuously in the indoor environments. Incorporation of moving boundary to the present geometry involves very complex modeling techniques, and procedures. We understand that this assumption will impose some constraints to the calculated results. For the well-mixed ventilation scenario, however, due to the relatively large airflow movement, we anticipate that the spatial and temporal concentration level calculated will not be affected significantly. The exposure level of the moving object can be estimated approximately by $\sum_x \int C_x(t)\mathrm{d}t$ where x represents the occupant location inside the domain. For the displacement ventilation, the buoyancy airflow inside the domain is induced primarily by the presence of the occupants. We anticipate that the results may not be as accurate as that of the well-mixed cases. It is understood that the majority of the exposure occurs during the droplet cloud first "hitting" the receiver. Due to high emission speed, the exposure time for the droplet plume passing the receiving occupant is very brief comparing to the moving time of the occupant, the current results are still expected to be acceptable.

4. Conclusions

A computational geometry for studying droplet dispersion under well-mixed and displacement ventilations was built. Droplet dispersion for two source-to-receiver orientations, i.e. face-to-face and face-to-wall, were analyzed via three different emission velocities namely 20, 50 and 100 m/s. Based on the results, despite their case dependency, some general conclusions can be drawn.

First of all, under the well-mixed scheme, dispersion is always approaching homogeneous. Second, under the displacement scheme, due to the low y-component air velocity, poor lateral dispersion is resulted and droplet-free regions are observed. Besides, the formation of the vertical plumes favors the droplet removal without causing substantial mixing inside the domain. Third, the ultimate concentration profile depends on the relaxation time, emission velocity, and ventilation scheme.

The degree of mixing was further quantified by the coefficient of variation. Due to the low global airflow in the computational domain, the CVs for displacement ventilation were found consistently higher than those for well-mixed ventilation. For practicality, proper installations of air-cleaning devices are also highlighted. In order to achieve higher removal efficiency, the device should be installed close to the exhaust outlet at high ceiling.

Acknowledgement

The work described in this paper was partially supported by a grant from CityU 7002273.

References

[1] N.E. Klepeis, W.C. Nelson, W.R. Ott, J.P. Robinson, A.M. Tsang, P. Switzer, J.V. Behar, S.C. Hern, W.H. Engelmann, The National Human Activity Pattern Survey (NHAPS): a resource for assessing exposure to environmental pollutants, J. Expo. Sci. Environ. Epidemiol. 11 (2001) 231–252.
[2] P. Xu, J. Peccia, P. Fabian, J.W. Martyny, K.P. Fennelly, M. Hernandez, S.L. Miller, Efficacy of ultraviolet germicidal irradiation of upper-room air in inactivating airborne bacterial spores and mycobacteria in full-scale studies, Atmos. Environ. 37 (2003) 405–419.
[3] C.B. Beggs, P.A. Sleigh, A quantitative method for evaluating the germicidal effect of upper room UV fields, J. Aerosol Sci. 33 (2002) 1681–1699.
[4] C.Y.H. Chao, M.P. Man, G.N. Sze To, Transport and removal of expiratory droplets in hospital ward environment, Aerosol Sci. Technol. 412 (2008) 377–394.
[5] L. Morawska, Droplet fate in indoor environments, or can we prevent the spread of infection? Indoor Air 15 (2006) 335–347.
[6] M. Nicas, W.W. Nazaroff, A. Hubbard, Toward understanding the risk of secondary airborne infection: emission of respirable pathogens, J. Occup. Environ. Hyg. 2 (2005) 143–154.
[7] N.P. Gao, J. Niu, P. Heiselberg, M. Perino, The airborne transmission of infection between flats in high-rise residential buildings: particulate simulation, Build. Environ. 44 (2009) 402–410.
[8] H. Qian, Y. Li, P.V. Nielsen, C.E. Hyldgaard, Dispersion of exhalation pollutants in a two-bed hospital ward with a downward ventilation system, Build. Environ. 43 (2008) 344–354.
[9] G.N. Sze To, M.P. Wan, C.Y.H. Chao, G. Wei, S.C.T. Yu, J.K.C. Kwan, A methodology for estimating airborne virus exposures in indoor environments using the spatial distribution of expiratory aerosols and virus viability characteristics, Indoor Air 18 (2008) 425–438.
[10] A.C.K. Lai, Y.C. Cheng, Study of expiratory droplet dispersion and transport using a new Eulerian modeling approach, Atmos. Environ. 41 (2007) 7473–7484.
[11] Y. Li, G.M. Leung, J.W. Tang, X. Yang, C.Y.H. Chao, J.Z. Lin, J.W. Lu, P.V. Nielsen, J. Niu, H. Qian, A.C. Sleigh, H.-J.J. Su, J. Sundell, T.W. Wong, P.L. Yuen, Role of ventilation in airborne transmission of infectious agents in the built environment—a multidisciplinary systematic review, Indoor Air 17 (2007) 2–18.
[12] T. Chang, Y. Hsieh, H. Kao, Numerical investigation of airflow pattern and particulate matter transport in naturally ventilated multi-room buildings, Indoor Air 16 (2006) 136–152.
[13] G. He, X. Yang, J. Srebric, Removal of contaminants released from room surfaces by displacement and mixing ventilation: modeling and validation, Indoor Air 15 (2005) 367–380.
[14] Q. Chen, L. Glicksman, System Performance Evaluation and Design Guidelines for Displacement Ventilation, ASHRAE, Atlanta, GA, 2003.
[15] American Society of Heating, Refrigerating and Air-Conditioning Engineers, Handbook: Fundamental, ASHRAE, Atlanta, 2005.
[16] M.P. Wan, C.Y.H. Chao, Transport characteristics of expiratory droplets and droplet nuclei in indoor environments with different ventilation airflow patterns, J. Biomech. Eng. Trans. ASME 129 (2007) 341–353.
[17] R. Tellier, Review of aerosol transmission of Influenza A virus, Emerg. Infect. Dis. 12 (2006) 1657–1662.
[18] W. Sun, J. Ji, Y. Li, X. Xie, Dispersion and settling characteristics of evaporating droplets in ventilated room, Build. Environ. 42 (2007) 1011–1017.
[19] X. Xie, Y. Li, A.T.Y. Chwang, P.L. Ho, W.H. Seto, How far droplets can move in indoor environments–revisiting the Wells evaporation–falling curve, Indoor Air 17 (2007) 211–225.

[20] W.F. Wells, Airborne Contagion and Air Hygiene, Harvard University Press, Cambridge, Massachusetts, 1955.
[21] S. Zhu, S. Kato, J.-H. Yang, Study on transport characteristics of saliva droplets produced by coughing in a calm indoor environment, Build. Environ. 41 (2006) 1691–1702.
[22] B. Zhao, Z. Zhang, X. Li, Numerical study of the transport of droplets or particles generated by respiratory system indoors, Build. Environ. 40 (2005) 1032–1039.
[23] H. Brohus, P.V. Nielsen, Personal exposure in displacement ventilated rooms, Indoor Air 6 (1996) 157–167.
[24] F. Chen, S.C.M. Yu, A.C.K. Lai, Modeling particle distribution and deposition in indoor environments with a new drift-flux model, Atmos. Environ. 40 (2006) 357–367.
[25] A.C.K. Lai, K. Wang, F. Chen, Experimental and numerical study on particle distribution in a two-zone chamber, Atmos. Environ. 42 (2008) 1717–1726.
[26] A.C.K. Lai, W.W. Nazaroff, Modeling indoor particle deposition from turbulent flow onto smooth surfaces, J. Aerosol Sci. 31 (2000) 463–476.
[27] T. Hussein, K. Hameri, M.S.A. Heikkinen, K. Markku, Indoor and outdoor particle size characterization at a family house in Espoo-Finland, Atmos. Environ. 39 (2005) 3697–3709.
[28] C.M. Long, H.H. Suh, P.J. Catalano, P. Koutrakis, Using time-and size-resolved particulate data to quantify indoor penetration and deposition behavior, Environ. Sci. Technol. 35 (2001) 2089–2099.
[29] B. Zhao, J. Wu, Modeling particle deposition from fully developed turbulent flow in ventilation duct, Atmos. Environ. 40 (2006) 457–466.
[30] B. Zhao, J. Wu, Modeling particle deposition onto rough walls in ventilation duct, Atmos. Environ. 40 (2006) 6918–6927.
[31] J.B. Wang, A.C.K. Lai, A new drift-flux model for particle transport and deposition in human airways, J. Biomech. Eng. Trans. ASME 128 (2006) 97–105.
[32] W.S. Dols, G.N. Walton, CONTANW 2.0 User Manual, National Institute of Standards and Technology, Maryland, 2000.
[33] H.E. Feustel, COMIS – an international multizone air-flow and contaminant transport model, Energy Build. 30 (1999) 3–18.
[34] W.W. Nazaroff, G.R. Cass, Mathematical modeling of indoor aerosol dynamics, Aerosol Sci. Technol. 23 (1989) 157–166.
[35] W.W. Nazaroff, M. Nicas, S.L. Miller, Framework for evaluating measures to control nosocomial tuberculosis transmission, Indoor Air 8 (1998) 205–218.
[36] D.T. Mage, W.R. Ott, Accounting for nonuniform mixing and human exposure in indoor environments, in: The Characterizing Sources of Indoor Air Pollution and Related Sink Effects, ASTM STP 1287, American Society for Testing and Materials, 1996, pp. 263–278.
[37] N. Gao, J. Niu, L. Morawska, Distribution of respiratory droplets in enclosed environments under different air distribution methods, Build. Simul. 1 (2008) 326–335.
[38] T.L. Thatcher, A.C.K. Lai, R. Moreno-Jackson, R.G. Sextro, W.W. Nazaroff, Effects of room furnishings and air speed on particle deposition rates indoors, Atmos. Environ. 36 (2002) 1811–1819.
[39] A.C.K. Lai, M.A. Byrne, A.J.H. Goddard, Experimental studies of the effect of rough surfaces and air speed on aerosol deposition in a test chamber, Aerosol Sci. Technol. 36 (2002) 973–982.